

Original Article

**Advantages of laserphyrin compared with photofrin in photodynamic therapy
for bile duct carcinoma**

Takashi Nonaka¹, Atsushi Nanashima¹, Mihoko Nonaka², Masataka Uehara²,
Hajime Isomoto³, Yoshikazu Nonaka¹, and Takeshi Nagayasu¹

Division of Surgical Oncology,¹ Department of Surgery, Department of Regenerative
Oral Surgery,² and Department of Gastroenterology and Hepatology,³ Nagasaki
University Graduate School of Biomedical Sciences, 1-7-1 Sakamoto, Nagasaki,
8528501 Japan

Running title: PDT with Laserphyrin for biliary carcinoma

Address for correspondence and requests for reprints:

Atsushi Nanashima, M.D.,

Division of Surgical Oncology, Department of Surgery, Nagasaki University Graduate
School of Biomedical Sciences, 1-7-1 Sakamoto, Nagasaki 852-8581, Japan.

Tel: +81 95 819 7304 Fax: +81 95 819 7306 E-mail: a-nanasm@net.nagasaki-u.ac.jp

Grant support: This investigation was supported by Grants-in-Aid for Scientific Research from the Ministry of Education (#21591777), Science, Sports and Culture of Japan.

No disclaimer and conflict of interest

Abstract

Background The aim of this study was to compare the effects of laserphyrin-PDT (L-PDT) on biliary cancer with those of conventional photosensitizer, photofrin-PDT (P-PDT).

Methods An animal tumor model was established by inoculation of NOZ cells in 4-week-old male BALB/c mice. The laser light wavelength was set at 630 nm for P-PDT and 660 nm for L-PDT, at a frequency of 10 Hz. Each group received a total energy fluence of 60 J/cm². The proportion of TUNEL (terminal deoxynucleotidyl transferase-mediated dUTP-biotin nick-end labeling)-positive cells, expression of VEGF (vascular endothelial growth factor) and the PCNA (proliferating cell nuclear antigen)-labeling index (LI) were assessed after PDT.

Results L-PDT had a significantly more potent apoptotic effects at 48 and 72 hours after light exposure compared with P-PDT ($P < 0.001$). The mean PCNA-LI was significantly lower in L-PDT group than P-PDT group and the index was significantly lower at several time points after PDT (6, 12, 24, 48 and 72 hours after laser light exposure) in the L-PDT than P-PDT ($P < 0.001$ vs control). The cell proliferative activity was significantly decreased at 12 and 24 hours after P-PDT than the control ($P < 0.001$). VEGF expression was significantly higher at 3 hours after L-PDT compared with the control ($P < 0.05$), whereas it was significantly higher at many time points after P-PDT (3, 6, 48 and 72 hours, $P < 0.05$ vs control).

Conclusions L-PDT is a better approach for biliary cancer than the conventional P-PDT based on the potent apoptotic and cytostatic effects.

Key Words Bile duct carcinoma • Photodynamic therapy • Laserphyrin • Local ablation • Apoptosis

Introduction

Photodynamic therapy (PDT) is based on the use of light to activate photosensitizers and induce cytotoxicity in adjacent tissue. PDT has become technically feasible and useful modality for the treatment of non-resectable cholangiocarcinoma.¹⁻⁵ In two randomized controlled trials, PDT provided longer survival than bile duct stenting alone.^{6,7} A possible explanation for the improved survival is the powerful anti-tumor immunological response induced by PDT.⁸ Our group has also reported the benefits of PDT treatment in bile duct carcinoma as chemotherapy or adjuvant chemotherapy after surgery for local control.⁹ The latest review on PDT for unresectable cholangiocarcinoma indicates that in most patients, PDT results in reductions in bilirubin serum level, improvement of quality of life, and prolongation of survival time, and that it has a few complications only.¹⁰

The first clinically-approved photosensitizer, hematoporphyrin derivative such as photofrin, was effective for treatment of cholangiocarcinoma.¹ However, this agent has various clinical drawbacks. For example, while it is effective in shallow bile duct wall epithelial tumors, it is less effective in tumors located in the deep layers.¹¹ Furthermore, the significantly long period of skin photosensitivity requires the patients to be kept away from strong sunlight for several weeks after drug administration.¹¹ Thus, a high tissue penetration and low skin photosensitivity are desirable in any new photosensitizing agents.

Mono-L-aspartyl chlorine6 (NPe6, talaporfin sodium, laserphyrin) is a second generation photosensitizer. It has certain advantages compared with photofrin. For

example, the 664 nm laser light used for laserphyrin penetrates tissue deeper than the 630 nm laser light used for photofrin.¹² Furthermore, laserphyrin-PDT (L-PDT) is associated with lower skin phototoxicity compared with photofrin¹³, and NPe6 is degraded rapidly *in vivo* and has excellent anti-tumor activity.^{12, 14} Moreover, L-PDT is effective in tumors even in the presence of bile, and has no serious hepatotoxicity.¹⁵ Thus, L-PDT is a promising treatment with higher cure rate and lower side effects than photofrin-PDT (P-PDT).¹⁶ We reported previously that P-PDT induces rapid apoptosis of human biliary cancer cells.¹⁷ However, to our knowledge, there is little or no information on the effect of L-PDT on biliary cancer. Based on its effect in other cancers, we hypothesized that L-PDT is more effective with more potent anti-tumor properties and reduced photosensitivity in bile duct cancer compared to P-PDT. To test our hypothesis, we compared the cytotoxic and angiogenic effects of L-PDT and P-PDT using a biliary cancer cell line (NOZ), a tumor model of bile duct cancer. Specifically, we employed the terminal deoxynucleotidyl transferase-mediated nick and labeling (TUNEL) assay to assess the extent of apoptosis, used the proliferating cell nuclear antigen (PCNA) labeling index (LI) to determine cell proliferation activity, and quantified the expression of vascular endothelial growth factor (VEGF) as an index of oxygenation of tumor tissue.

Materials and methods

In vitro studies of the properties of photosensitizers

Cell culture

NOZ cells, a human biliary cancer cell line (JCRB1033: Japanese Collection of Research Bioresources, Tokyo, Japan), were cultured in Dulbecco's modified Eagle medium (DMEM: Nissui Central Co., Tokyo) with 10% fetal bovine serum, glutamine (0.6 mg/ml), penicillin (100 units/ml) and streptomycin (100 mg/ml) at 37°C under a humidified atmosphere of 5% CO₂ in air.

Photodynamic therapy

NOZ cells were exposed to the specified levels of Photofrin® (Lederle Japan Co., Tokyo) and Laserphyrin® (Meiji Seika, Tokyo) for 24 hours and irradiated with an Nd:YAG pumped dye laser (Quanta-Ray DCR-3 and PDL-2, Spectra Physics, Mountain View, CA) tuned to a wavelength of 630 nm for P-PDT and 660 nm for L-PDT, which was verified with a spectrometric multi-channel analyzer (SMA Systems, Tokyo Instruments, Tokyo), at a frequency of 10 Hz (energy density range: 4.0 to 16.0 J/cm²). The estimated dose of P-PDT was 5, 10 and 20 µg/ml, while that of L-PDT was 10, 20 and 50 µg/ml. The photosensitizer was washed out of the cell culture medium with phosphate-buffered saline (PBS), and sensitizer-free fresh medium was added before irradiation.

Cell viability assay

The effect of PDT on NOZ cell viability was investigated with methyl-tetra-zolium (MTT; 3[4, 5-dimethyl-thiazoyl-2-yl] 2,5-diphenyl-tetrazolium bromide (Sigma, St. Louis, MO). Cells were cultured onto 96-well microplates and irradiated for 24 hours, and 10 µl of MTT solution (5 mg MTT per 1 ml PBS) was added to each well, followed by incubation for 4 hours. Finally, 100 µl acid-isopropanol was added to each well to solubilize MTT-formazan. After complete solubilization of the dye by vortexing the plate, absorbance was read on an Immunoreader (model NJ-2000, Nihon Inter Med, Tokyo) at 570 nm.

Staining for apoptosis

Cells were stained with Hoechst 33342 dye (Sigma), as a marker of apoptosis, at 24 hours after PDT to detect chromatin condensation and fragmentation under 50% lethal dose (LD₅₀) conditions in both groups (Fig. 1a, b).

Animal experiments

Tumor xenograft

In these experiments, 1×10^7 NOZ cells were inoculated subcutaneously into the back of 4-week-old nude mice (n=60, BALB/cANcrj nu/nu, Charles River Inc., Japan).

Tumors that grew to approximately 8×8 mm in approximately 21 days after inoculation (n=60) were used as the experimental model.

PDT protocol

Laser was tuned to a wavelength of 630 nm (P-PDT) and 660 nm (L-PDT); verified with a spectrometric multi-channel analyzer, at a frequency of 10 Hz. A power meter (30 A-P Ophir Optics, Jerusalem, Israel) was used to measure the light intensity.

Laserphyrin and photofrin were injected intraperitoneally into BALB/cANcrj nu/nu mice. The time interval between photosensitizer injection and light exposure for laserphyrin (10 mg/kg) and photofrin (7 mg/kg) was 2 and 24 hours, respectively.

Each tumor received a total energy fluence of 60 J/cm². During laser light exposure, the animals were anesthetized with intraperitoneally-injected pentobarbital sodium (40 mg/kg body weight). In the L-PDT group (n=28) and P-PDT group (n=28), PDT was directed to the transplanted tumor on the back of the animal. Mice were sacrificed at 0, 3, 6, 12, 24, 48 and 72 hours after PDT. Neither the photosensitizer nor laser light was used in the control animals (n=4).

Measurement of tumor necrotic area

Four mice each were sacrificed by ether inhalation at 24 h after continuous PDT. The tumors were excised and fixed in 3.7% neutral buffered formalin for 24 h, followed by processing for routine paraffin embedding. Three 4- μ m sections were prepared from each specimen, mounted on silanized slides (DAKO Japan Co.), and dried overnight on a hot plate at 37°C to promote adhesion. The first section from each of the specimens was stained with hematoxylin and eosin (H&E). In each specimen, the tumor necrotic area was measured using computer-assisted image analysis software

(Macintosh Image v1.62). The proportion of the necrotic area relative to the total cross-sectional tumor area was computed.¹⁸

TUNEL assay

TUNEL assay was performed using an Apoptosis Detection Kit (Wako, Osaka, Japan) in accordance with the instructions provided by the manufacturer. Slides were assessed under a light microscope, and TUNEL-positive nuclei (stained deep brown, Fig. 2a, b) were counted in three randomly selected microscopic fields ($\times 400$, i.e., field size: 0.08 mm^2) per slide with necrotic areas, and were expressed as the percentage of total nuclei counted. At least 1,000 nuclei were counted in each slide.

Immunohistochemistry for PCNA

PCNA immunohistochemical staining (ABC Kit, Vector Laboratories, Burlingame, CA) was carried out (n=4 for each group, Fig. 2c, d, e) using mouse anti-PCNA monoclonal antibody (PC10, dilution 1:100, Dako, Glostrup, Denmark). Sections incubated with normal mouse serum instead of PCNA served as negative controls. Both the labeled and unlabeled tumor cells were counted with the aid of a squared eyepiece reticule (Nikon, Tokyo) ($0.0625 \text{ mm}^2/\text{field}$) at a magnification of X400. The PCNA-LI of tumor cells was defined as the percentage of PCNA-positive cells among 1,000 tumor cells counted in three randomly selected fields.

VEGF immunohistochemistry

VEGF immunohistochemical staining (ABC Kit, Vector Laboratories) was performed as described below (n=4 for each group, Fig. 2f, g, h). Tissue sections were deparaffinized and rehydrated in water. Sections were treated with 0.1% trypsin solution in 0.05 M Tris buffer (pH 7.6) at room temperature for 15 min, followed by washing in PBS three times. Endogenous peroxidase was inhibited by treatment with 0.3% H₂O₂ in methanol for 30 min. After three washes with PBS, the sections were incubated overnight at 4°C with anti-human VEGF polyclonal antibody (dilution 1:200, #A-20, Santa Cruz Biotechnology, Santa Cruz, CA) in PBS, followed by incubation with diluted biotinylated secondary antibody for 30 min, and ABC reagent for 30 min. Immunohistochemical reactions were developed with diaminobenzidine (DAB) solution (20 mg in 100 ml 0.05 M Tris buffer containing 17 µl of 30% H₂O₂). The sections were counterstained lightly with Mayer's hematoxylin. Negative controls, prepared by substituting normal goat serum for the primary antibody, resulted in no detectable staining.

VEGF expression was expressed as the percentage of VEGF-immunopositive area (PVIA), which was quantified by computer-assisted image analysis (Macintosh Image, v1.62). The sections were photographed using a Nikon digital camera (Coolpix 4500, Nikon Co., Tokyo), at X50 magnification. After saving the captured image from three randomly selected fields in a personal computer, the image was cropped to 512 X512 pixels. After noise reduction and edge enhancement, the image was analyzed using the method of Wu et al.¹⁹ and the PVIA was determined for each specimen.

Statistical analysis

Data are expressed as mean \pm SD. Statistical significance was determined by two-way multi-repeated ANOVA, one-way factorial ANOVA and multiple comparison tests by Scheffe's test using the statistical package StatView (Abacus Concepts Inc., Berkeley, CA). Furthermore, the Mann–Whitney U-test was used for evaluation of percentages of stained cells. A *P* value less than 0.05 was considered statistically significant.

Results

In vitro studies

Effect of PDT on NOZ cell viability

Viability was determined by the MTT assay at 24 hours after PDT in each condition. The anti-tumor activity of PDT against NOZ cells was clearly seen with 10 µg/ml of photofrin and 20 µg/ml of laserphyrin, and the survival curves for P-PDT and L-PDT were similar. Cell death was induced in a light dose-dependent manner in both P-PDT and L-PDT groups (Fig. 3a, b). To induce LD₅₀ PDT conditions, a laser power of 12 J/cm² was required for NOZ. Induction of NOZ cell apoptosis in each group was investigated after treatment under LD₅₀ conditions (Fig. 1a, b).

Animal studies

Histological findings

In the control specimens, several mitotic tumor cells were observed, with only a few necrotic areas in the tumors. Complete disappearance of the tumor cells was not observed in the P-PDT and L-PDT groups, and histological findings at 0 and 3 h after PDT were similar to those of the control group (no laser light). Tumor cells with nuclear condensation appeared at 6 h after PDT. The area of tumor necrosis increased gradually with time after PDT, although many surviving tumor cells were still present, mainly in the peripheral areas of each specimen. There was no difference in the necrotic area at 24 hours after laser light application between the PDT and L-PDT groups in experiments using 7 mg/kg P-PDT and 10 mg/kg L-PDT (P=0.68, Fig. 4).

Induction of apoptosis

The percentage of apoptotic cells in the tumor tissue was significantly different between the P-PDT and L-PDT groups ($P < 0.001$) (Fig. 5a). TUNEL-positive cells began to increase significantly in the inoculated tumor from 6 hours after PDT in the L-PDT group, and from 12 hours after PDT in the P-PDT group. The percentage of apoptotic cells was significantly higher in the L-PDT group than the P-PDT at both 48 and 72 hours after laser light exposure ($P < 0.001$).

Proliferative activity of tumor cells

The mean PCNA-LI of the control group was 50.9%. In general, the mean PCNA-LI was lower in the two PDT groups than the control throughout the observation period. There were significant differences in PCNA-LI between the P-PDT and L-PDT groups ($P < 0.001$, Fig. 5b), with a significantly lower PCNA-LI in the L-PDT group ($32.2 \pm 4.9\%$) than the P-PDT group ($44.4 \pm 7.0\%$, $P < 0.001$) and the control ($50.9 \pm 7.2\%$, $P < 0.001$) at 6 hours after laser application. However, there was no significant difference in PCNA between the two groups at 12, 24 and 48 hours after laser light application (Fig. 5b, $P = 0.82$). Interestingly, the mean PCNA-LI was significantly lower in the L-PDT group ($26.7 \pm 7.9\%$) than the P-PDT group at 72 h after PDT ($45.9 \pm 4.0\%$, $P < 0.001$).

Effect of PDT on VEGF expression

The percentage of VEGF-positive area (PVIA) at 3 hours after PDT was significantly larger in the L-PDT group ($18.0 \pm 6.7\%$) compared with the control group ($8.2 \pm 3.5\%$,

$P=0.0016$), though it gradually decreased thereafter. The PVIA at 72 h ($10.0\pm 2.5\%$) was equivalent to that of the control group ($8.2\pm 3.5\%$, $P=0.99$). On the other hand, the PVIA at 3, 6, 48 and 72 h after PDT was larger for the P-PDT group compared with the control group (control: 8.2 ± 3.5 , P-PDT: $15.3\pm 2.9\%$ at 3 h, $19.0\pm 3.9\%$ at 6 h, $16.8\pm 6.4\%$ at 48 h, and $16.0\pm 3.4\%$ at 72 h, $P<0.05$). The PVIA was significantly smaller in the L-PDT group than the P-PDT at 6, 48 and 72 hours after laser light exposure ($P<0.05$). However, there were no significant differences in PVIA between the P-PDT and L-PDT groups at the different time intervals after PDT ($P=0.12$, Fig. 5c).

Discussion

In the present study, we compared the cytotoxic effects of P-PDT and L-PDT on biliary cancer cells. Previous studies showed that the main effect of PDT is apoptosis of the cultured cells, evidenced by assays measuring either the fragmentation of DNA or chromatin condensation.^{20,21} In the present *in vitro* study, PDT induced death of NOZ cells in a light dose-dependent manner and apoptotic bodies were found in Hoechst 33342-stained sections at LD50 conditions.

In our *in vivo* study, irradiation was applied under similar laser power condition. Fig. 4 shows the results of preliminary experiment designed to select the concentration of drug required to achieve an equivalent anti-tumor effect. The anti-tumor effect was assessed by measuring the area of necrosis in H&E stained sections. The extent of apoptosis, PCNA-L.I. and PVIA were compared under similar conditions. Our *in vivo* study showed a more potent induction of apoptosis by L-PDT compared with P-PDT at 48 hours after laser light application. It has been reported that PDT has direct cytotoxic effect as well as indirect effects on the tumor microenvironment.²⁰ PDT rapidly induces apoptosis, inflammatory reaction, tumor-specific and/or -non-specific immune reactions and damage of the microvasculature of the tumor bed.^{20,22,23} The mechanism of PDT-induced apoptosis may vary according to the type of cells being treated, the type of photosensitizer used, the light delivery protocol employed, and the time lag between photosensitizer and light treatment.^{24,25} Usuda et al.²⁶ reported the involvement of enhanced apoptotic response, as evidenced by the high ratio of Bax and Bcl-2 protein, in LLC-IL-6 cells

and that the expression of IL-6 is an important determinant of the antitumor effect of L-PDT. It is possible that changes in the tumor microenvironment (inflammatory reaction, tumor-specific and/or -non-specific immune reactions) related to differences in the photosensitizers are the main reason for the different rate of apoptosis between P-PDT and L-PDT noted in the present study.

PCNA is a 36-kDa nuclear polypeptide involved in cell proliferation.²⁷ In the present study, we used the PCNA-LI to evaluate tumor growth activity since it is reported that PCNA synthesized during the late G1-to-S phase is an auxiliary for DNA polymerase.²⁸ Our results showed a more profound suppression of cancer cell proliferation activity in the L-PDT group than the P-PDT group. Furthermore, the results demonstrated a low PCNA-LI at the early phase in the L-PDT group compared with the P-PDT group. In this regard, Song et al.²⁹ reported that NPe6 at the dosages studied promoted greater tumor regression than HpD with a long lasting inhibitory effect on tumor growth in a human cholangiocarcinoma model. It was also reported that NPe6-PDT induced complement activation with subsequent expression of various leukotrienes and mediators, including cytokines IL-6, which were responsible for the observed neutrophilia.³⁰ In addition, LLC-IL-6 cells are reported to be more sensitive to PDT than the parental LLC and LLC-Neo cells.²⁶ Based on these findings, it is possible that the above changes in the immune system may mediate the suppressive actions of L-PDT on the re-growth of residual tumors and its early-to-late cytostatic effects, compared with P-PDT.

Photochemical reactions depend on the level of oxygen in tumor tissues.³¹ However, PDT induces severe tumor tissue hypoxia immediately after its application,

which is linked to the induction of photochemical reaction.³² VEGF production is induced in cells under hypoxic conditions³³ and other stresses.³⁴ Ferrario et al³⁵ reported that the reduced vascular perfusion associated with PDT-mediated injury of the microvasculature produced tumor tissue hypoxia, which, in turn, induced VEGF expression via activation of the hypoxia-inducible factor-1 (HIF-1) transcription factor. Thus, expression of VEGF can be used as an index of tumor tissue oxygenation. In the L-PDT group, it is conceivable that the observed overexpression of VEGF at 0 and 3 h after PDT was likely due to hypoxia induced by photochemical reactions.

Experimental evidence suggests that the expression of VEGF in hypoxic cells returns gradually to the baseline level upon resumption of oxygen supply to the affected tissues.³³ In comparison, in the P-PDT group, VEGF expression did not return to the baseline though it increased at 3 and 6 hours. Jiang et al³⁶ demonstrated immunohistochemically an increase in VEGF expression within the PDT-treated lesions at 7 days after P-PDT and remained elevated for a few weeks. Considered together, these findings suggest prolonged tumor tissue hypoxia in the P-PDT compared with L-PDT, probably due to a more pronounced effect of vascular occlusion in P-PDT. As discussed above, tumor tissue hypoxia induces the production of various angiogenesis factors such as VEGF. Consequentially, it is hypothesized that L-PDT produces more profound suppression of VEGF expression compared with P-PDT. In this regard, Ohtani et al³⁷ reported that high levels of GADD-45 α and VEGF expression were associated with tumor recurrence and cell survival via upregulation of IL-2. Overexpression of VEGF is thought to contribute to the “angiogenic switch” of the malignant phenotype in human cholangiocarcinoma.³⁸

Overexpression of VEGF (by estrogens for example) plays an important role in the regulation of growth of human cholangiocarcinoma.³⁹ Hida and coworkers⁴⁰ reported that VEGF is an independent predictor of survival in extrahepatic biliary tract carcinoma, though Möbius and colleagues⁴¹ found no correlation between VEGF-A expression and survival in extrahepatic cholangiocarcinoma. For these reasons, L-PDT causes a small or no increase in VEGF expression compared with P-PDT, and consequently, L-PDT could suppress angiogenesis and re-growth of the residual tumor.

In conclusion, the TUNEL assay used in the present study demonstrated significant differences in the effects of P-PDT and L-PDT. Furthermore, quantification of the PCNA-LI showed significant differences between the P-PDT and L-PDT groups at 6 hours after laser light. Furthermore, the percentage of the VEGF area was significantly larger in P-PDT than L-PDT at the early period after PDT application. Based on these results, the anti-tumor effects of L-PDT mediated through apoptosis are more significant than those of P-PDT. In addition, L-PDT is effective in preventing the recurrence of residual tumor due to the low potential of angiogenic response. Considered together, the results suggest that L-PDT can be regarded as a new generation treatment option for bile duct cancer.

References

1. McCaughan JS, Jr, Mertens BF, Cho C, Barabash, R. D, Payton, HW.
Photodynamic therapy to treat tumors of the extrahepatic biliary ducts. A case report. *Arch Surg* 1991; 126: 111-3.
2. Witzigmann H, Berr F, Ringel U, Caca K, Uhlmann D, Schoppmeyer K, et al.
Surgical and palliative management and outcome in 184 patients with hilar cholangiocarcinoma: palliative photodynamic therapy plus stenting is comparable to r1/r2 resection. *Ann Surg* 2006; 244: 230-9.
3. Ortner MA, Liebetruth J, Schreiber S, Hanft M, Wruck U, Fusco V, et al.
Photodynamic therapy of nonresectable cholangiocarcinoma. *Gastroenterology* 1998; 114: 536-42.
4. Berr F, Wiedmann M, Tannapfel A, Halm, U, Kohlhaw KR, Schmidt F, et al.
Photodynamic therapy for advanced bile duct cancer: evidence for improved palliation and extended survival. *Hepatology* 2000; 31: 291-8.
5. Rumalla A, Baron TH, Wang KK, Gores GJ, Stadheim LM, de Groen PC.
Endoscopic application of photodynamic therapy for cholangiocarcinoma. *Gastrointest Endosc* 2001; 53: 500-4.
6. Ortner ME, Caca K, Berr F, Liebetruth J, Mansmann U, Huster D, et al.
Successful photodynamic therapy for nonresectable cholangiocarcinoma: a randomized prospective study. *Gastroenterology* 2003; 125: 1355-63.

7. Zoepf T, Jakobs R, Arnold JC, Apel D, Riemann JF. Palliation of nonresectable bile duct cancer: improved survival after photodynamic therapy. *Am J Gastroenterol* 2005; 100: 2426-30.
8. Zoepf T. Photodynamic therapy of cholangiocarcinoma. *HPB (Oxford)* 2008; 10: 161-3.
9. Nanashima A, Yamaguchi H, Shibasaki S, Ide N, Sawai T, Tsuji T, et al. Adjuvant photodynamic therapy for bile duct carcinoma after surgery: a preliminary study. *J Gastroenterol* 2004; 39: 1095-101.
10. Fei Gao, Yu Bai, Shu-Ren Ma, Feng Liu, Zhao-Shen Li. Systematic review: photodynamic therapy for unresectable cholangiocarcinoma. *J Hepatobiliary Pancreat Sci* 2010; 17: 125–31.
11. Gomer C J, Rucker N, Ferrario A, Wong S. Properties and applications of photodynamic therapy. *Radiat Res* 1989; 120: 1-18.
12. Roberts WG, Shiau FY, Nelson JS, Smith KM, Berns MW. *In vitro* characterization of monoaspartyl chlorin e6 and diaspartyl chlorin e6 for photodynamic therapy. *J Natl Cancer Inst* 1988; 80: 330-6.
13. Ferrario A, Kessel D, Gomer CJ. Metabolic properties and photosensitizing responsiveness of mono-L-aspartyl chlorin e6 in a mouse tumor model. *Cancer Res* 1992; 52: 2890-3.
14. Roberts WG, Smith KM, McCullough JL, Berns MW. Skin photosensitivity and photodestruction of several potential photodynamic sensitizers. *Photochem Photobiol* 1989; 49: 431-8.

15. Kasuya K, Shimazu M, Suzuki M, Kuroiwa Y, Usuda J, Itoi T, et al. Novel photodynamic therapy against biliary tract carcinoma using mono-L-aspartyl chlorine e6: basic evaluation for its feasibility and efficacy. *J Hepatobiliary Pancreat Sci* 2010; 17: 313–21.
16. Kato H, Furukawa K, Sato M, Okunaka T, Kusunoki Y, Kawahara M, et al. Phase II clinical study of photodynamic therapy using mono-L-aspartyl chlorin e6 and diode laser for early superficial squamous cell carcinoma of the lung. *Lung Cancer* 2003; 42: 103-11.
17. Nonaka T, Nanashima A, Nonaka M, Uehara M, Isomoto H, Asahina I, et al. Analysis of apoptotic effects induced by photodynamic therapy in a human biliary cancer cell line. *Anticancer Res* 2010; 30: 2113-8.
18. Uehara M, Sano K, Wang ZL. Enhancement of the photodynamic antitumor effect by streptococcal preparation OK-432 in the mouse carcinoma. *Cancer Immunol Immunother* 2000; 49: 401-9.
19. Wu L C, D'Amelio F, Fox R A, Polyakov I, Dauntton NG. Light microscopic image analysis system to quantify immunoreactive terminal area apposed to nerve cells. *J Neurosci Methods* 1997; 74: 89-96.
20. Oleinick NL, Morris R L, Belichenko I. The role of apoptosis in response to photodynamic therapy: what, where, why, and how. *Photochem Photobiol Sci* 2002; 1: 1-21.
21. Luo Y, Chang C K, Kessel D. Rapid initiation of apoptosis by photodynamic therapy. *Photochem Photobiol* 1996; 63: 528-34.

22. Gomer C J, Ferrario A, Luna M, Rucker N, Wong S. Photodynamic therapy: combined modality approaches targeting the tumor microenvironment. *Lasers Surg Med* 2006; 38: 516-21.
23. Dougherty T J. An update on photodynamic therapy applications. *J Clin Laser Med Surg* 2002; 20: 3-7.
24. Dougherty T J, Gomer C J, Henderson B W, Jori G, Kessel D, Korbek M, et al. Photodynamic therapy. *J Natl Cancer Inst* 1998; 90: 889-905.
25. Ahmad N, Mukhtar H. Mechanism of photodynamic therapy-induced cell death. *Methods Enzymol* 2000; 319: 342-58.
26. Usuda J, Okunaka T, Furukawa K, Tsuchida T, Kuroiwa Y, Ohe Y, et al. Increased cytotoxic effects of photodynamic therapy in IL-6 gene transfected cells via enhanced apoptosis. *Int J Cancer* 2001; 93: 475-80.
27. Mathews MB, Bernstein RM, Franza BR, Jr, Garrels JI. Identity of the proliferating cell nuclear antigen and cyclin. *Nature* 1984; 309: 374-6.
28. Bravo R, Frank R, Blundell PA, Macdonald-Bravo H. Cyclin/PCNA is the auxiliary protein of DNA polymerase-delta. *Nature* 1987; 326: 515-7.
29. Wong Kee Song LM, Wang KK, Zinsmeister AR. Mono-L-aspartyl chlorin e6 (NPe6) and hematoporphyrin derivative (HpD) in photodynamic therapy administered to a human cholangiocarcinoma model. *Cancer* 1998; 82: 421-7.
30. Kobayashi W, Liu Q, Matsumiya T, Nakagawa H, Yoshida H, Imaizumi T, et al. Photodynamic therapy upregulates expression of Mac-1 and generation of leukotriene B(4) by human polymorphonuclear leukocytes. *Oral Oncol* 2004; 40: 506-10.

31. Moan J, Sommer S. Oxygen dependence of the photosensitizing effect of hematoporphyrin derivative in NHIK 3025 cells. *Cancer Res* 1985; 45: 1608-10.
32. Henderson B W, Fingar V H. Relationship of tumor hypoxia and response to photodynamic treatment in an experimental mouse tumor. *Cancer Res* 1987; 47: 3110-4.
33. Shweiki D, Itin A, Soffer D, Keshet E. Vascular endothelial growth factor induced by hypoxia may mediate hypoxia-initiated angiogenesis. *Nature* 1992; 359: 843-5.
34. Eyssen-Hernandez R, Ladoux A, Frelin C. Differential regulation of cardiac heme oxygenase-1 and vascular endothelial growth factor mRNA expressions by hemin, heavy metals, heat shock and anoxia. *FEBS Lett* 1996; 382: 229-33.
35. Ferrario A, von Tiehl KF, Rucker N, Schwarz MA, Gill PS, Gomer CJ. Antiangiogenic treatment enhances photodynamic therapy responsiveness in a mouse mammary carcinoma. *Cancer Res* 2000; 60: 4066-9.
36. Jiang F, Zhang Z G, Katakowski M, Robin AM, Faber M, Zhang F, et al. Angiogenesis induced by photodynamic therapy in normal rat brains. *Photochem Photobiol* 2004; 79: 494-8.
37. Ohtani K, Usuda J, Ichinose S, Ishizumi T, Hirata T, Inoue T, et al. High expression of GADD-45alpha and VEGF induced tumor recurrence via upregulation of IL-2 after photodynamic therapy using NPe6. *Int J Oncol* 2008; 32: 397-403.
38. Benckert C, Jonas S, Cramer T, Von Marschall Z, Schäfer G, Peters M, et al. Transforming growth factor beta 1 stimulates vascular endothelial growth factor

- gene transcription in human cholangiocellular carcinoma cells. *Cancer Res* 2003; 63: 1083–92.
39. Mancino A, Mancino MG, Glaser S, Alpini G, Bolognese A, Izzo L, et al. Estrogens stimulate the proliferation of human cholangiocarcinoma by inducing the expression and secretion of vascular endothelial growth factor. *Dig Liver Dis* 2008; 41: 156–63.
40. Hida Y, Morita T, Fujita M, Miyasaka Y, Horita S, Fujioka Y, et al. Vascular endothelial growth factor expression is an independent negative predictor in extrahepatic biliary tract carcinomas. *Anticancer Res* 1999; 19: 2257–60.
41. Möbius C, Demuth C, Aigner T, Wiedmann M, Wittekind C, Mössner J, et al. Evaluation of VEGF A expression and microvascular density as prognostic factors in extrahepatic cholangiocarcinoma. *EJSO* 2007; 33: 1025-9.

Figure legends

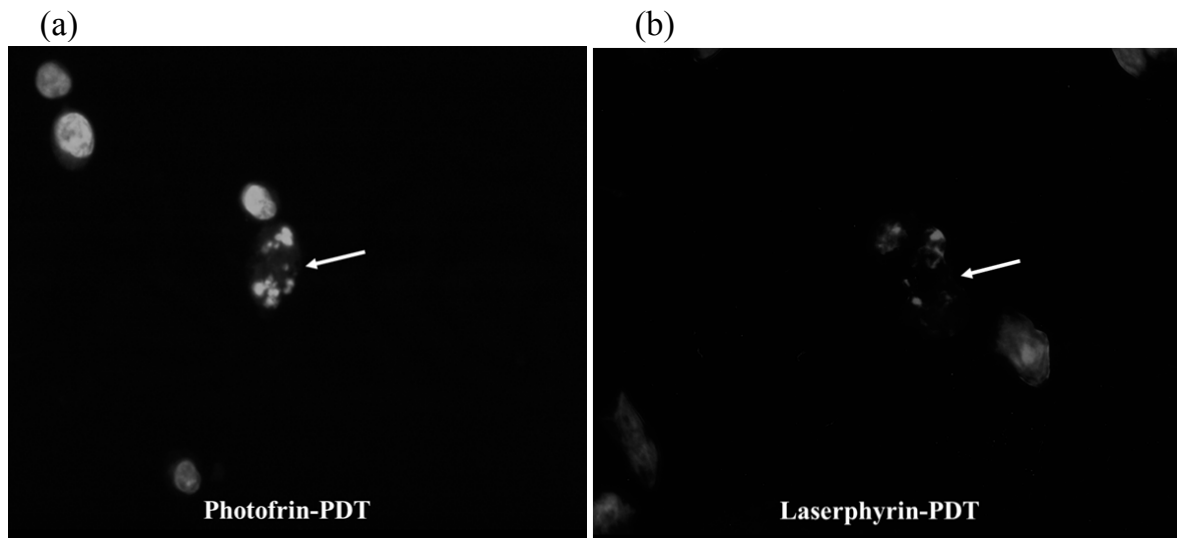


Figure 1. Fluorescence microscopy of cells stained with Hoechst33342 at 24 hours after (a) photofrin-PDT and (b) laserphyrin-PDT at LD₅₀ conditions. Arrows: apoptotic cells with nuclear condensation (original magnification X100).

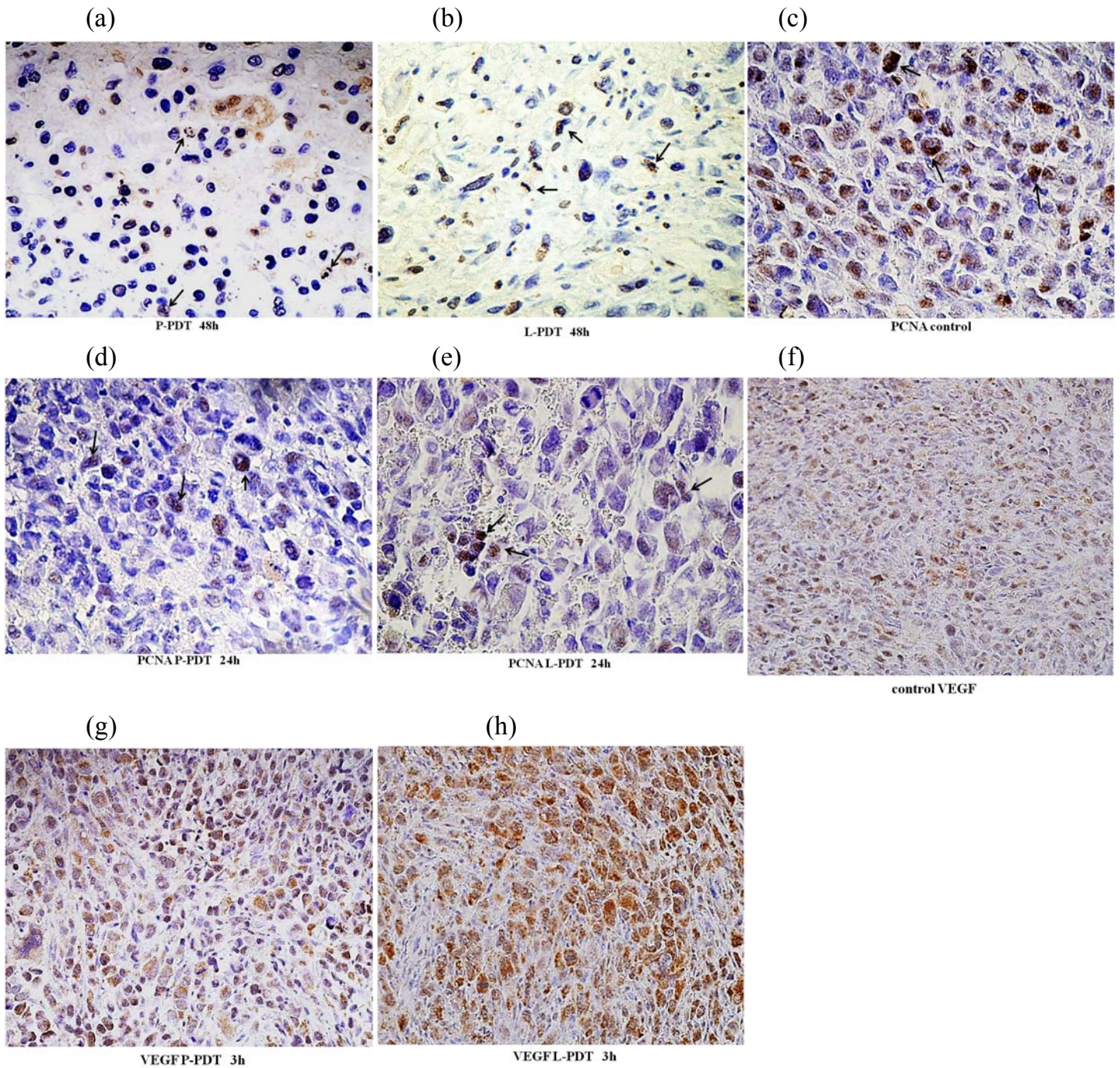


Figure 2. Induction of apoptosis by (a) P-PDT and (b) L-PDT at 48 h after PDT. Arrows: TUNEL-positive cells. (c-e) PCNA immunohistochemical staining. (c) control untreated tumor, (d) tumor at 6 h after P-PDT treatment, (e) tumor at 6 h after L-PDT treatment. Arrows: PCNA-labeled cells. (f-h) VEGF immunohistochemical staining. Note the deep brown staining of the cytoplasm of VEGF-positive cells. (f) Control untreated tumor, (g) tumor at 3 h after P-PDT treatment, (h) tumor at 3 h after L-PDT treatment.

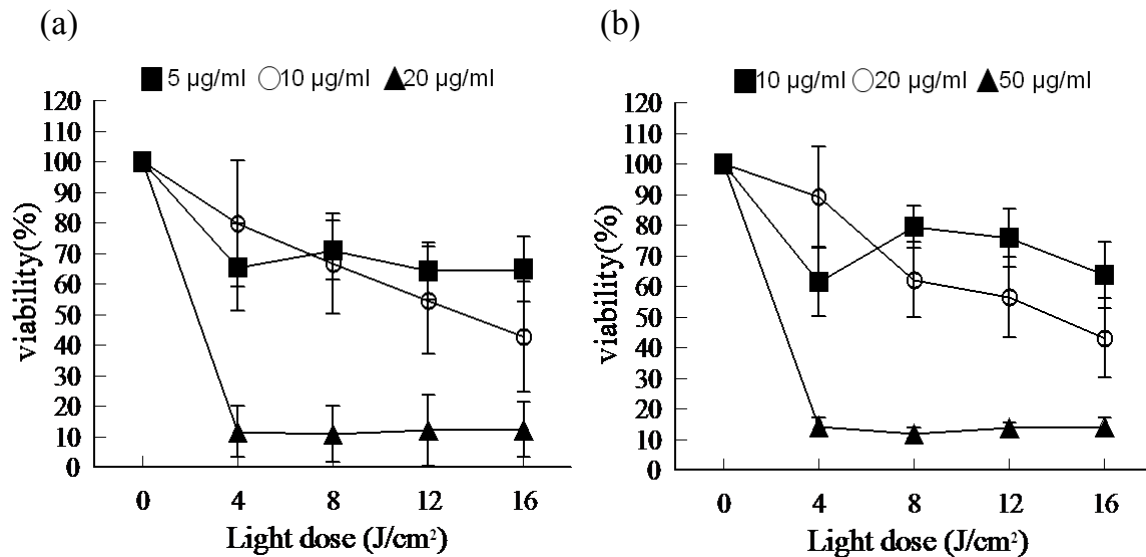


Figure 3. Effects of PDT on NOZ cell viability estimated at 24 hours after laser light application by MTT assay. (a) The estimated anti-tumor activity of PDT against NOZ cells was 10 µg/ml photofrin. Values are expressed as mean±SD and represent the average of three independent experiments. (b) The estimated anti-tumor activity of PDT against NOZ cells was 20 µg/ml laserphyrin. Values are expressed as mean±SD and represent the average of three independent experiments.

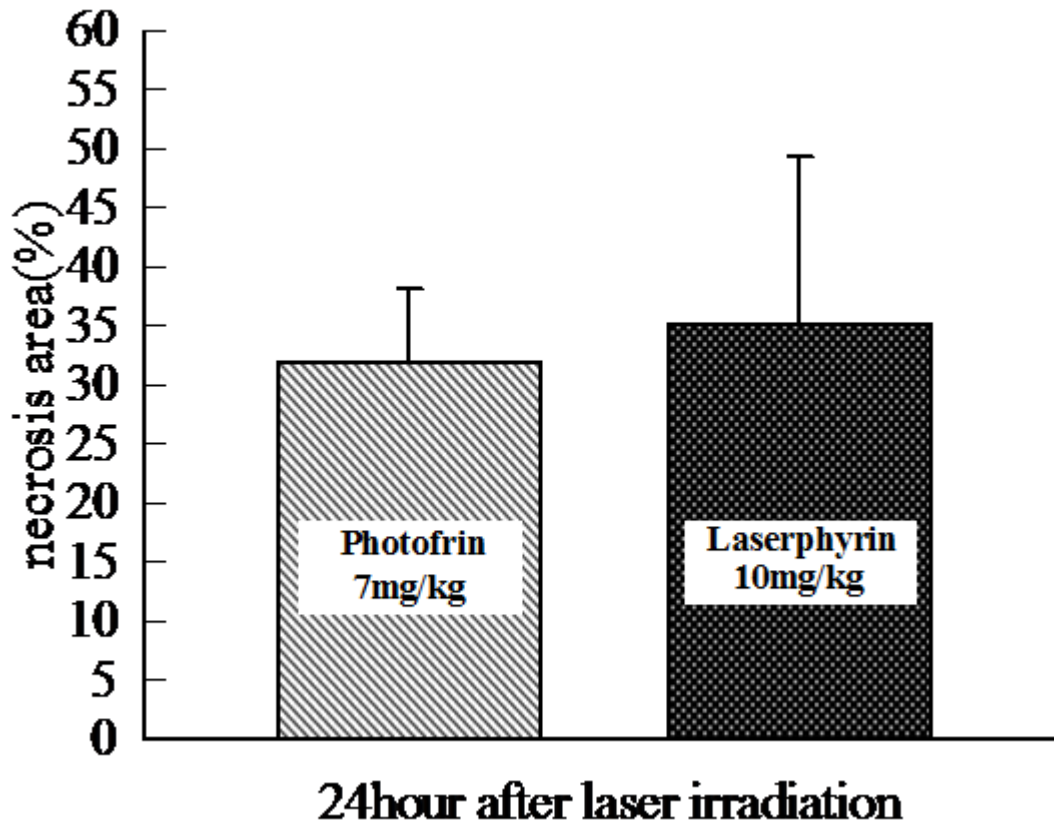


Figure 4. Mean percentage of necrotic tumor area after 7 mg/kg P-PDT and 10 mg/kg L-PDT estimated at 24 hours after laser light exposure. The difference in necrotic area was not significant between the two groups. Data are mean \pm SD. Checkered bars: P-PDT, solid bars: L-PDT.

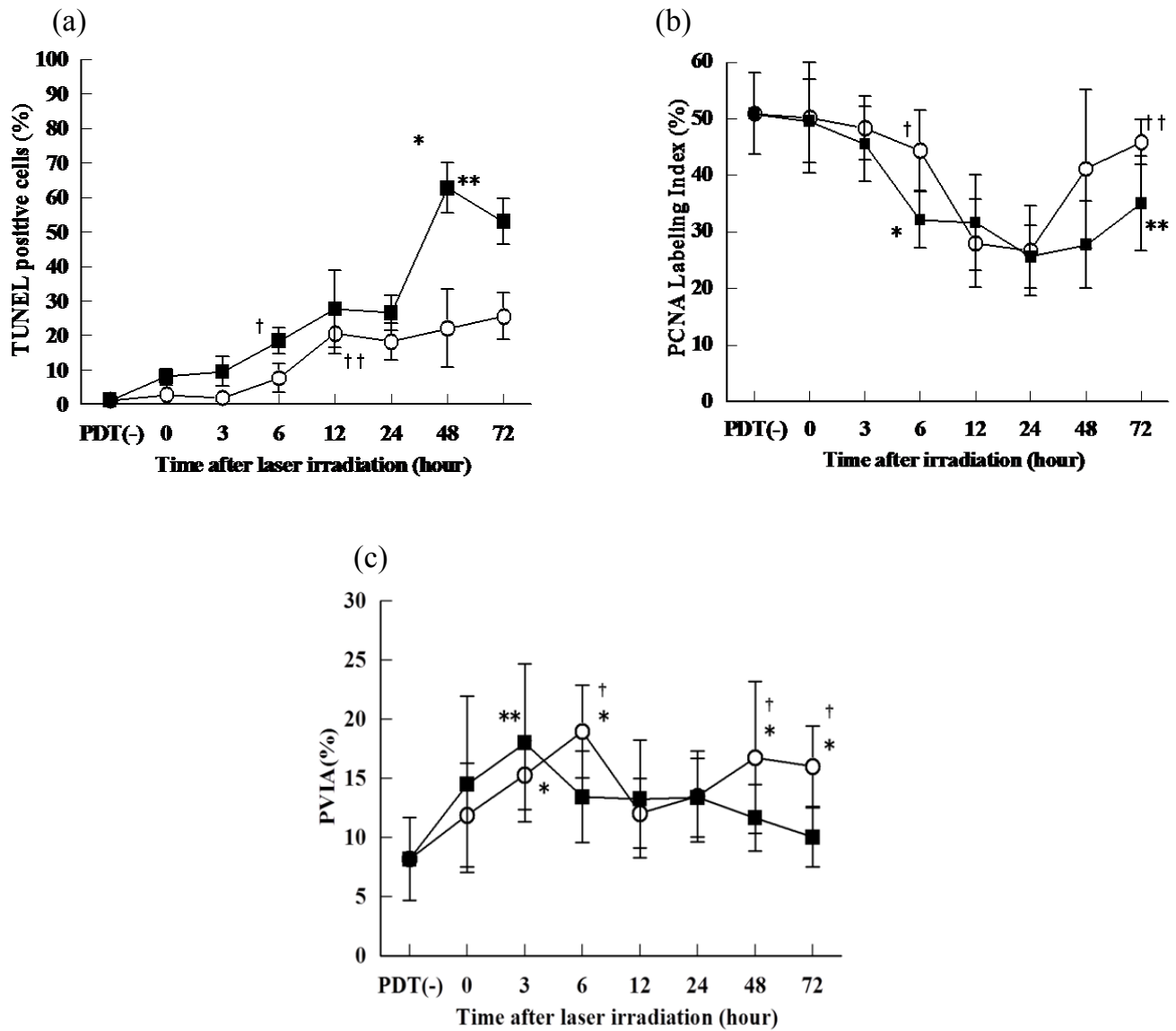


Figure 5. (a) Mean percentage of TUNEL-positive cells in each group. There was a significant difference between the P-PDT and L-PDT groups ($P < 0.001$). Data are mean \pm SD. * $P < 0.001$ P-PDT vs. L-PDT at 48 hours after laser light application. ** $P < 0.001$ P-PDT vs. L-PDT at 72 hours after laser light application. † $P < 0.001$ vs. the control group in L-PDT. †† $P < 0.001$ vs. the control group in P-PDT. Open circles: P-PDT, solid squares: L-PDT. (b) Proliferating cell nuclear antigen (PCNA) labeling index (LI) of tumor cells in each group. Data are mean \pm SD. There were significant differences between the P-PDT and L-PDT groups ($P < 0.001$), between the P-PDT and

L-PDT at 6 hours after laser light application ($P < 0.001$). $*P < 0.001$ vs. the control group in L-PDT, $\dagger P = 0.82$ vs. the control group in P-PDT. $**P = 0.17$ vs. 24 hours after laser light application in L-PDT, $\dagger\dagger P < 0.001$ vs. 24 hours after laser light application in P-PDT. Open circles: P-PDT, solid squares: L-PDT. (c) VEGF-immunopositive area of the control and experimental groups. Data are mean \pm SD. There was no significant difference between the P-PDT group and L-PDT group ($P = 0.123$). $**P = 0.0016$ vs. the control group in L-PDT, $*P < 0.05$ vs. the control group in P-PDT. $\dagger P < 0.05$ P-PDT vs. L-PDT at 6, 48 and 72 hours after laser light application. Open circles: P-PDT, solid squares; L-PDT.